

In Situ Measurements of the Complex Permittivity of Materials Using Reflection Ellipsometry in the Microwave Band: Experiments (Part II)

Florence Sagnard, Faroudja Bentabet, and Christophe Vignat

Abstract—The aim of this series of two papers is to propose a new experimental tool based on the reflection ellipsometry technique for *in situ* characterization of single-layer dielectric materials at microwave frequencies. In the first part of this paper [1], the theoretical part of the technique and the associated multistep numerical algorithm used to estimate the complex permittivity of a sample have been presented. In this second part, we focus on the experimental setup and on the results. We report the estimated values of the complex permittivity for several types of materials and compare them with results obtained by the Fresnel method. We show that measured values agree with those currently published.

Index Terms—Complex permittivity, ellipsometry, free-space methods, Fresnel coefficients, material characterization, microwave frequencies, polarization, reflexion.

I. INTRODUCTION

IN THIS second part, the experimental validation of the reflection ellipsometry technique, for *in situ* characterization of dielectric materials at microwave frequencies, as proposed in [1], is presented. In this context, we have designed an experimental setup named COTREMO, which includes an automated measurement system, allowing the retrieval of the powers reflected by the surface of the sample as a function of the rotation angle of the receiving antenna [2]. Each ellipsometric curve obtained is then analyzed by a numerical multistep method to deduce an estimate of the complex permittivity ($\tilde{\epsilon} = \epsilon' - j\epsilon''$) of a single-layer sample (whose thickness is assumed to be known) and its associated uncertainties.

Several common types of materials, such as a concrete wall, fiberboard, plasterboard, and PVC slabs, have been studied. Estimates of the complex permittivity have been obtained, first from ellipsometry, then from two other methods: the Fresnel method (an alternate free-space technique) and a guided method using a coaxial structure. We show that the different measurement values are included in ranges reported in the literature [3]–[9]. Moreover, for each sample, the complex permittivity issued from reflection ellipsometry has been studied as a function of the angle of incidence for frequencies included in the X and Ku bands.

Manuscript received May 11, 2004; revised September 13, 2004. This work was supported by the French Department of Research (ANVAR).

F. Sagnard is with the Université de Marne-La-Vallée, Cité Descartes, 77454 Marne-La-Vallée Cedex 02, France, and with INSA de Rennes, IETR, 35043 Rennes Cedex, France (e-mail: florence.sagnard@insa-rennes.fr).

F. Bentabet and C. Vignat are with the Université de Marne-La-Vallée, Cité Descartes, 77454 Marne-La-Vallée Cedex 02, France.

Digital Object Identifier 10.1109/TIM.2005.847199

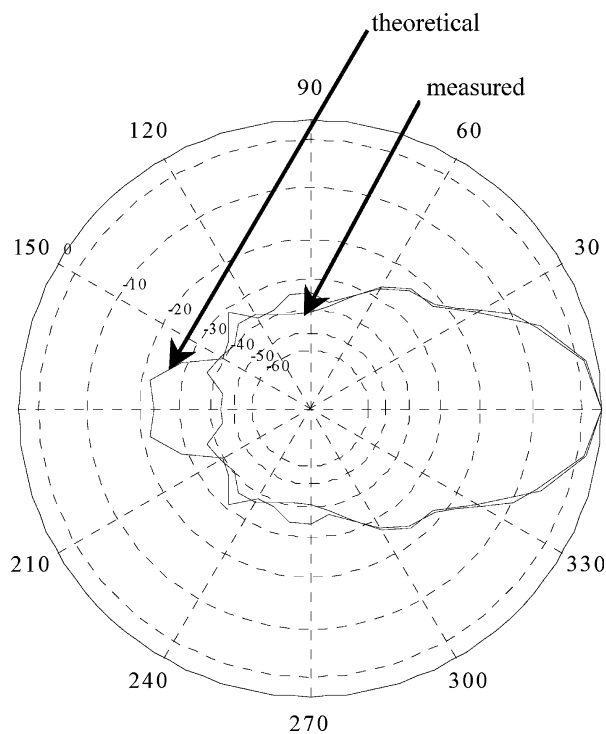


Fig. 1. Experimental and theoretical radiation patterns of one X-band horn antenna in the H-plane.

In Section II, a description of the experimental setup COTREMO and of the experimental conditions is given. Then, the main experimental results are synthesized in Section III. We provide three types of results: i) the analysis of the ellipsometric curves associated with different angles of incidence and with different frequencies, ii) the estimations of the complex permittivity for each sample considering several experimental conditions, and iii) comparisons with results issued from alternate measurement techniques. Section IV is dedicated to concluding remarks and future prospects.

II. EXPERIMENTAL SETUP

A. General Description

The experimental measurement system, depicted in [1, Fig. 1], allows measuring the reflected waves in free-space in the frequency bands X and Ku, using either the Fresnel method or ellipsometry. The overall system is built on a semicircular horizontal plane support made up of plexiglass and placed in front of the material under test. A bistatic configuration is used.

Two pairs of horn antennas associated with both bands have been used. Each antenna is set on a column (at 70 cm above the basis) fixed on an arm, allowing the adjustment of the radius R (1 m for the Fresnel method and 0.6 m for ellipsometry) of the support which marks out the angle of incidence. A waveguide adapter which fills the rotating system allows the rotation (described by the angle A) of the receiving antenna around its symmetry axis. For alignment, each column has rotation and translation capabilities. The pyramidal horns have been chosen with particularly low phase deviation at their aperture (for example, 19.5° for E-plane and 54° for H-plane in X band). The overall measured far-field 3-dB beamwidth of the electrical field, for both polarizations and both bands, is near 30° . Fig. 1 shows the measured and theoretical values of the radiating pattern of the X-band antennas in the H-plane configuration [10]. An incident power of 12 dBm is generated for each frequency belonging to the X or Ku band, and a low power detector [-20 dBm; -70 dBm] has been chosen.

To cancel scattering phenomena from the sample, its size has been chosen greater than the first Fresnel zone at the grazing incidence ($1 \text{ m} \times 2 \text{ m}$). In order to focus the two antennas on the same footprint on the surface of the sample, a narrow laser beam positioned at the center of each antenna has been used. Depending on each of the methods, Fresnel or ellipsometry, experimental conditions such as the distance R between the antenna and the spot of reflection have been chosen for an optimal detection.

B. Specific Physical Phenomena

We have calculated, as a function of the angle of incidence θ_i , the width of the Fresnel ellipsoid associated with the first Fresnel zone and, particularly at the lower frequencies where it is larger. This evaluation helps us to determine the minimal dimensions of the sample that prevent diffraction effects at the edges; we have compared the major axis a' of this Fresnel zone with the footprint of the radiated field generated by the antenna (see Fig. 2). Assuming that the distance R between the antennas and the spot of reflection on the sample surface is large compared to the wavelength λ , the major a' and minor axis b' of the Fresnel ellipse express thus as a function of the angle of incidence as follows:

$$\begin{aligned} a' &= \sqrt{\frac{\lambda R^2}{2R \cos^2 \theta_i + \lambda}} \\ b' &= \sqrt{\frac{\lambda R}{2}}. \end{aligned} \quad (1)$$

Consequently, at a fixed frequency, the overall angle β from which the receiving antenna sees the major axis of the ellipse evolves with the angle of incidence θ_i as

$$\beta = a' \tan \left(\frac{a' \sin \theta_i}{R - a' \cos \theta_i} \right) + a' \tan \left(\frac{a' \cos \theta_i}{R - a' \sin \theta_i} \right). \quad (2)$$

This angle increases with the angle of incidence θ_i : There exists a limit value of the angle of incidence (called the limit angle) above which the overall 3-dB beamwidth is smaller than the antenna angle-of-sight of the first Fresnel zone; in such case, the detected power is not typical of the physical phenomena involved. Considering the two experimental conditions chosen

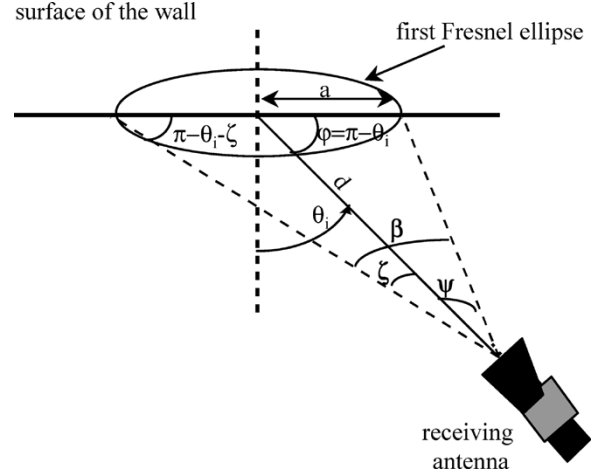


Fig. 2. Influence of the angle of incidence on the width of the first Fresnel zone.

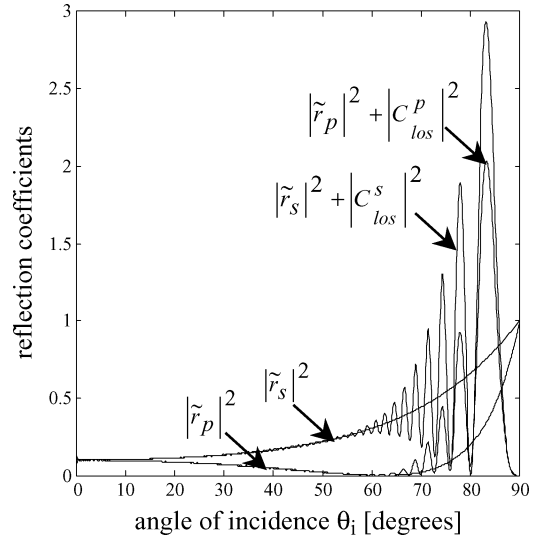


Fig. 3. Contribution of the line-of-sight wave path for the parallel (p) and perpendicular (s) polarizations in the case of an infinite thickness sample ($\tilde{\epsilon}_r = 3.5 - j$, $F = 10$ GHz, $R = 1$ m).

for our measurement comparisons, either $R = 1$ m at $F = 10$ GHz or $R = 0.6$ m at $F = 8.5$ GHz, the limit angles of incidence are evaluated to 70.4° and 58.4° , respectively.

We have also considered the influence of the radiating pattern on the power received by the antenna. The contribution of the line-of-sight path to the received power can be expressed by the following formula:

$$\begin{aligned} |C_{\text{LOS}}|^2 &= \frac{G^2 \left(\frac{\pi}{2} - \theta_i \right)}{\sin \theta_i} \left[\frac{G^2 \left(\frac{\pi}{2} - \theta_i \right)}{\sin \theta_i} \right. \\ &\quad \left. + 2|\tilde{r}_{p,s}| \cos \left(\varphi - \frac{4\pi R}{\lambda_0} (1 - \sin \theta_i) \right) \right] \end{aligned} \quad (3)$$

where $G(\pi/2 - \theta_i)$ is the gain of the receiving antenna in the direction $(\pi/2 - \theta_i)$ [10] and $\varphi = \omega(\tau_{\text{LOS}} - \tau_d) = (2R/c)(\sin \theta_i - 1)$ is the phase deviation between the line-of-sight and the reflected wave path.

Considering the two measurement configurations, it appears from Fig. 3 that the interference generated by the reflected and line-of-sight signals becomes significant beyond the angle of incidence $\theta_i = 70^\circ$.

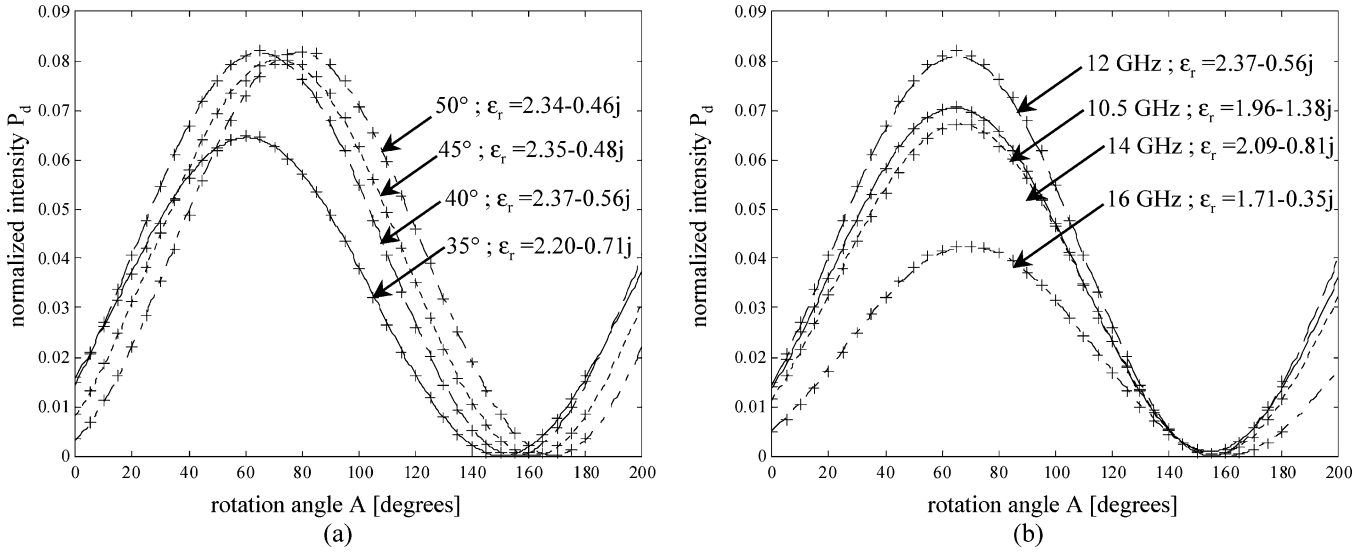


Fig. 4. Experimental ellipsometric curves in the case of the 12-mm-thick plasterboard sample for different values of (a) the angle of incidence ($F = 12$ GHz) and (b) the frequency ($\Theta_i = 45^\circ$).

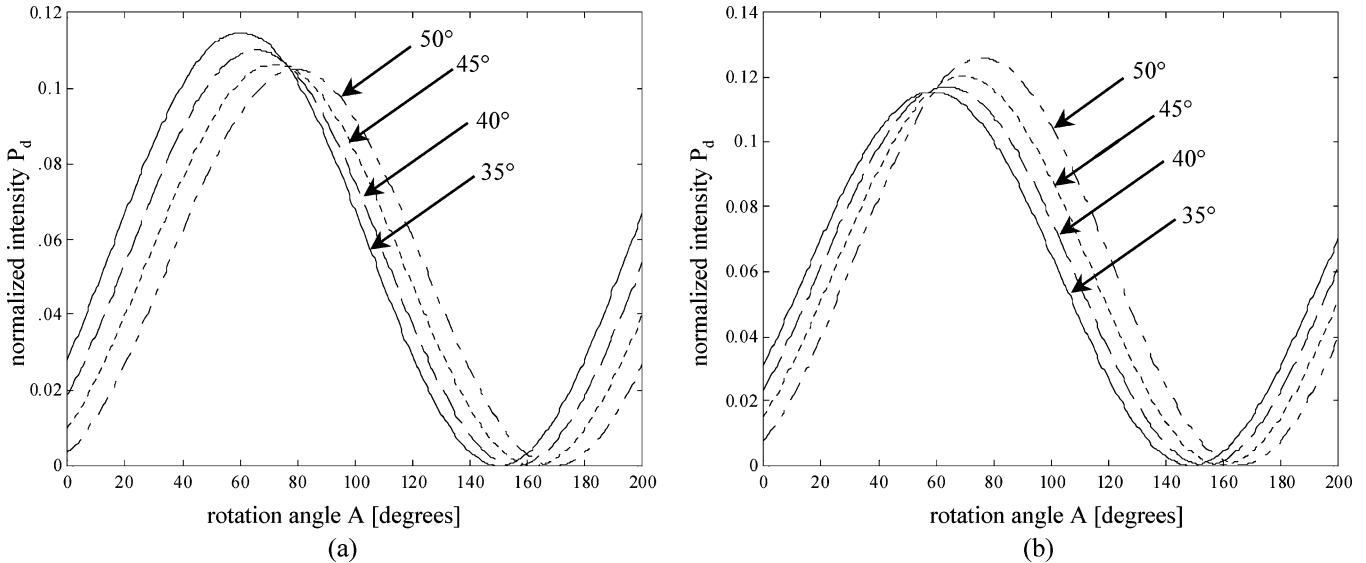


Fig. 5. Study of the shape variation of theoretical ellipsometric curves ($F = 12$ GHz, $\Delta z = 12$ mm) in the vicinity of the reference value $\epsilon_r = 2.32 - 0.55j$. Cases (a) $\epsilon_r = 2.32 - 0.1j$ and (b) $\epsilon_r = 2.7 - 0.55j$.

III. COMPLEX PERMITTIVITY ESTIMATIONS ON SEVERAL SAMPLES

A. Experimental Conditions

Several samples like a concrete wall [$e = 19.5$ cm (M1)], a fiberboard [$e = 10$ mm (M2) and 16 mm (M3)], plasterboard [$e = 12$ mm (M4)], and PVC slabs [$e = 10.4$ mm (M5) and 15.5 mm (M6)] have been characterized in reflection at different frequencies included in the X and Ku bands. Materials are supposed to be homogenizable (their inclusions are small compared to the wavelength or they are stratified): To verify the dielectric homogeneity of the sample and the planeness of the wave front, we have checked that, for a given angle of incidence and a given polarization, the measured reflection coefficients remain constant (up to the measurement uncertainties) when considering different antenna to wall distances R and different positions of the spot on the sample. Their relative complex permittivity

$\tilde{\epsilon}_r$ has been estimated at different angles of incidence θ_i and frequencies F using reflection ellipsometry in the ranges $[35^\circ; 50^\circ]$ and $[8.5$ GHz; 17 GHz], respectively. The maximal uncertainties associated with the measured reflected power P_d and the analyzer angle A are, respectively, estimated to the following average values: ± 0.2 dB (relative) and $\pm 0.3^\circ$ (absolute); they represent the maximum deviation obtained during the integration time of each scalar measurement.

B. Experimental Ellipsometric Curves

As an example, in the case of the 12-mm-thick plasterboard sample (M4), experimental ellipsometric curves have been plotted on Fig. 4, first as a function of the angle of incidence (at frequency 12 GHz) and secondly as a function of the frequency (at the angle of incidence 40°); the rotation angle A of the receiving antenna varies in the range $[0; 180^\circ]$. For each

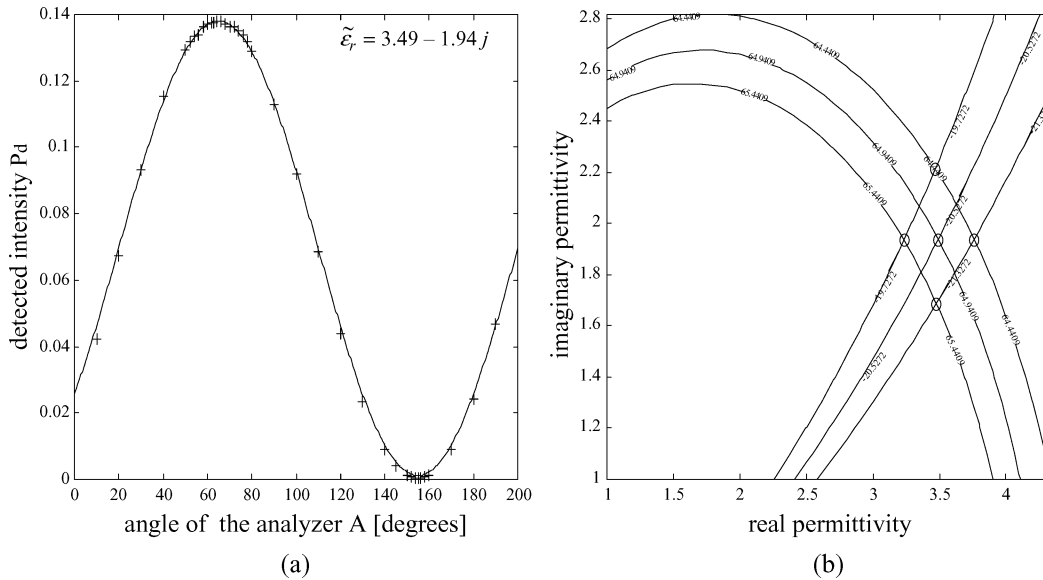


Fig. 7. Estimation of the complex permittivity using reflection ellipsometry in the case of a concrete wall of large thickness ($F = 8.5$ GHz, $\Theta_i = 45^\circ$).

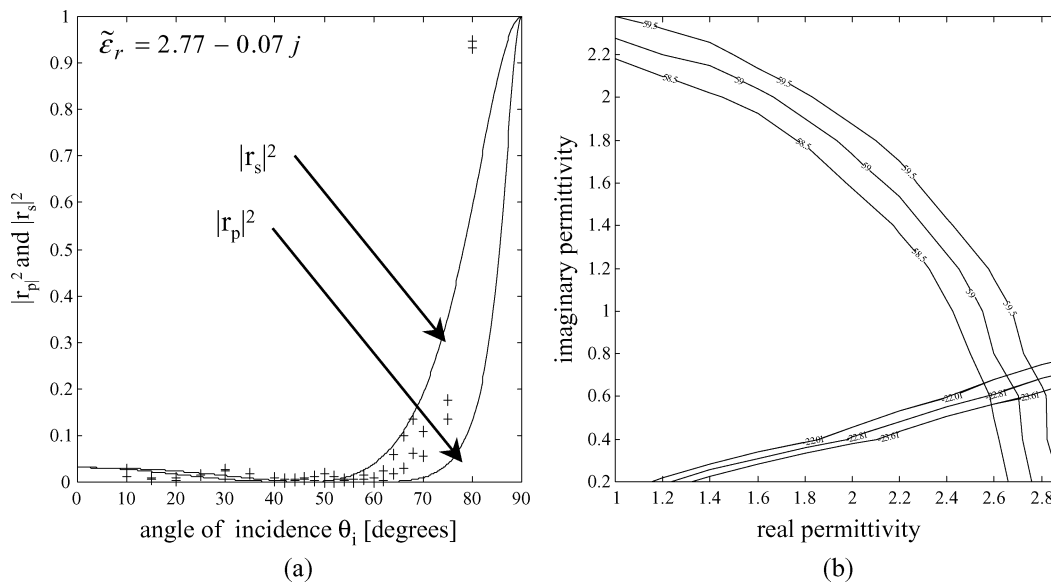


Fig. 8. Estimation of the complex permittivity using the Fresnel method in the case of a fiberboard sample of thickness 10 mm ($F = 10$ GHz).

A theoretical parameter study has thus been performed to understand in more detail the physical phenomena involved. This study shows that a slight variation of the complex permittivity makes the ellipsometric curves to different frequencies more distant from each other.

C. Comparisons of the Fresnel and Reflection Ellipsometry Methods

Estimations of the complex permittivity issued from the two methods have been compared for two types of samples supposed to be thick or thin compared to the wavelength, in the X band. For this comparison, the experimental conditions of each method have been optimized.

1) *Concrete Wall (Thick Sample)*: In this case, we consider a sample which is thick (19.5 cm) compared to the wavelength. The reflection coefficients and their ratio, as measured by the

Fresnel method, are plotted as a function of the angle of incidence θ_i on Fig. 6. Using a nonlinear least squares approach to fit either jointly both reflection coefficients or their ratio, yields estimated permittivities equal, respectively, to $\tilde{\epsilon}_r = 3.55 - 1.19j \pm (0.15 - 0.07j)$ and $\tilde{\epsilon}_r = 3.47 - 1.23j \pm (0.15 - 0.07j)$ at $F = 10$ GHz. These estimated values of permittivity appear very close. We underline that the mean uncertainties of free-space measurements associated with the values of ϵ' and ϵ'' are evaluated to less than 10% and around 20% (case of small values of ϵ''), respectively. The large deviations between the measured data and the theoretical curves appearing for both extreme (small and large) values of the angle of incidence can be explained by the nonnegligible effect of the line-of-sight path in these extreme configurations. It must be underlined that in this method, the first estimate of the complex permittivity is determined by the coordinates of the minimum extracted from a

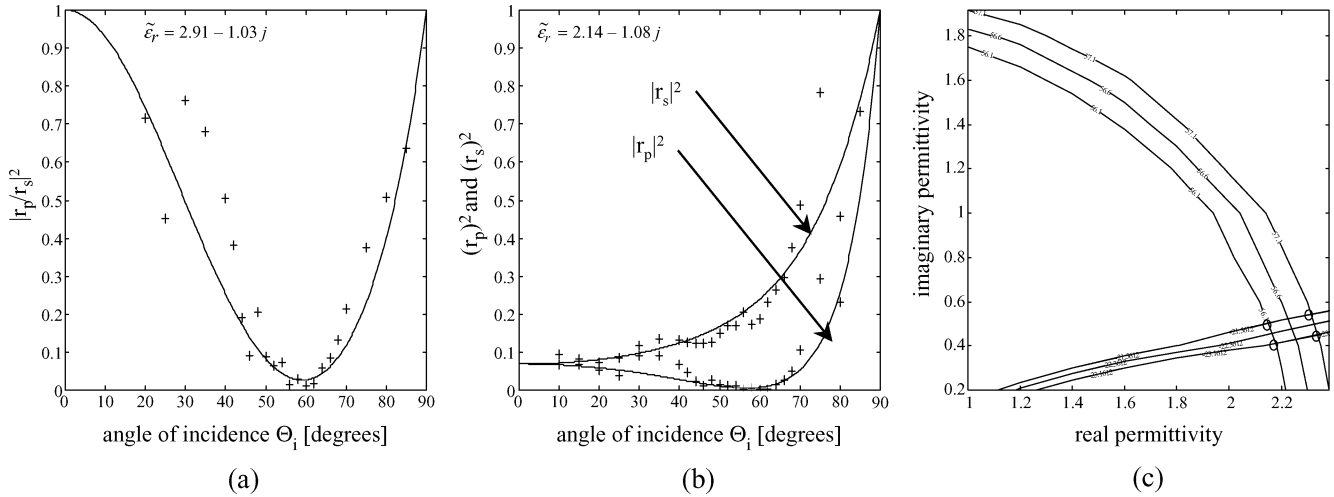


Fig. 9. Estimation of the complex permittivity using the Fresnel method in the case of a fiberboard sample of thickness 16 mm ($F = 10$ GHz) by two approaches ($F = 10$ GHz): (b) the individual reflection coefficients [and the corresponding parallelogram of uncertainties (c)] and (a) their ratio.

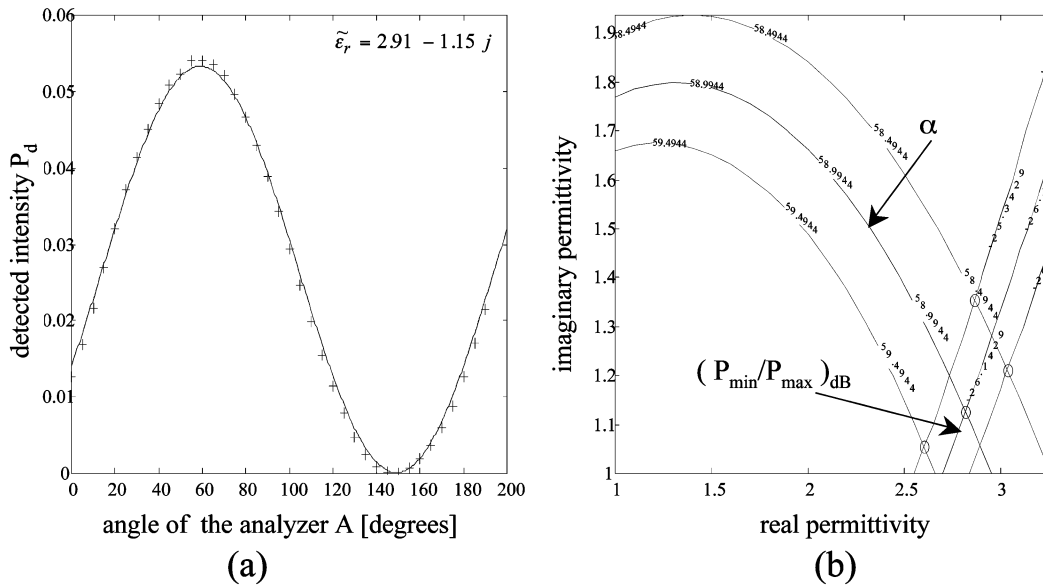


Fig. 10. Estimation of the complex permittivity using ellipsometry in the case of a fiberboard sample of thickness 10 mm ($F = 8.5$ GHz, $\Theta_i = 35^\circ$).

fitting of the experimental curve of the ratio of both reflection coefficients made only in its vicinity.

In the case of the ellipsometry method, with $\theta_i = 45^\circ$, the measured data follow almost exactly a raised sine-shaped curve, as shown in Fig. 7. Taking into account the measurement uncertainties, the theoretical curve fitting at best the data corresponds to an estimated complex permittivity value of $\tilde{\epsilon}_r = 3.49 - 1.94j \pm (0.26 - 0.26j)$ at $F = 8.5$ GHz. In this case, the uncertainties are estimated from the two parameters $(P_{\min}/P_{\max})_{\text{dB}}$ and α , deduced from the fitting of the experimental curve. We remark that these values of permittivity are close to those determined by the Fresnel method and that they belong to the range of those appearing in the literature [6].

As a conclusion, the values of the complex permittivity of the concrete wall issued from both Fresnel and ellipsometry methods appear close. We observe that, in both cases, the measurement data fit satisfactorily the theoretical curves. The uncertainties on the real and imaginary parts of the complex per-

mittivity appear larger in the ellipsometry method than in the Fresnel method, but they should be more representative of reality since in the Fresnel approach, the direct path received by the receiving antenna cannot be assumed constant when the angle of incidence changes.

2) *Fiberboard (Thin Sample)*: Because the thicknesses of the two different fiberboard samples are small compared to the wavelength (for example, $\lambda_0 = 3.5$ cm at 8.5 GHz), absorbing materials have been placed far behind the samples. In the case of the Fresnel method, and considering only the optimal joint fit of both reflection coefficients, the estimated permittivities are, for the 10- and 16-mm-thick slabs, $\tilde{\epsilon}_r = 2.77 - 0.85j \pm (0.13 - 0.09j)$ and $\tilde{\epsilon}_r = 2.14 - 1.08j \pm (0.1 - 0.07j)$, respectively, at $F = 10$ GHz (see Figs. 8 and 9).

In the case of ellipsometry, the experimental curves, as shown in Figs. 10 and 11, yield the following estimated permittivities for the 10- and 16-mm slab (with $\theta_i = 35^\circ$ and $\theta_i = 45^\circ$, respectively): $\tilde{\epsilon}_r = 2.91 - 1.15j \pm (0.22 - 0.23j)$ and

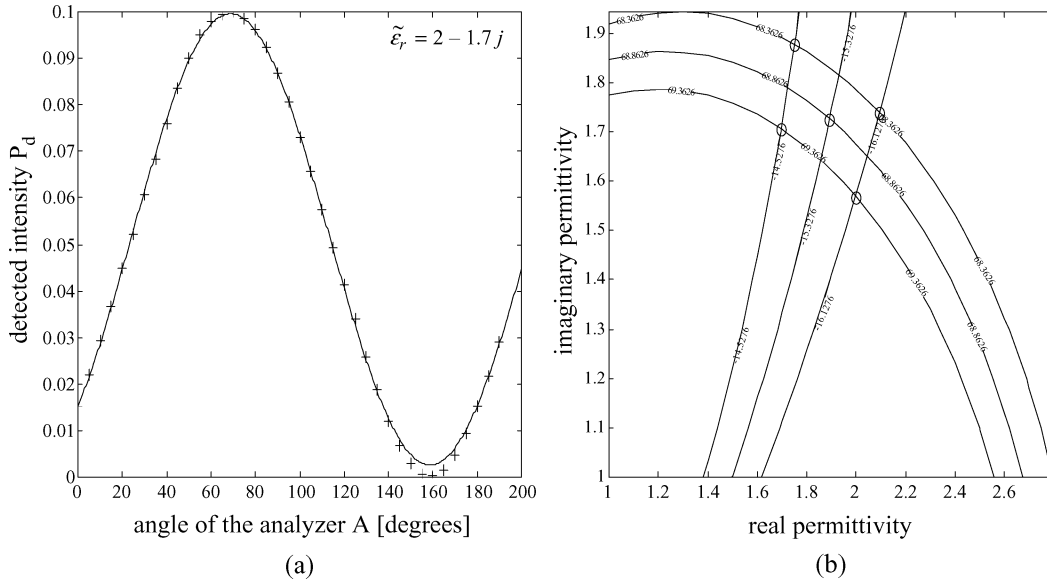


Fig. 11. Estimation of the complex permittivity using ellipsometry in the case of a fiberboard sample of thickness 16 mm ($F = 8.5$ GHz, $\Theta_i = 45^\circ$).

TABLE I
VALUES OF COMPLEX PERMITTIVITIES AVERAGED OVER FOUR ANGLES ON INCIDENCE [35° ; 40° ; 45° ; 50°] ASSOCIATED WITH THE DIFFERENT SAMPLES

materials	Frequencies			
	8.5 GHz	12 GHz	14 GHz	18 GHz
PVC 15.5mm	2.92-0.92j	2.19-1.13j	2.14-0.82j	2.18-0.4j
PVC 10.4mm	1.85-1.04j	2.6-0.95j	2.86-0.43j	2.92-0.89j
fiberboard 16mm	2-0.61j	2.47-0.67j	2.22-1.01j	2.59-0.62
fiberboard 10mm	2.32-1.2j	2.33-1.01j	2.93-0.75j	3.5-0.66j
plasterboard 12mm		2.32-0.55j	2.09-0.55j	2.04-1.61j

$\tilde{\epsilon}_r = 2 - 1.7j \pm (0.2 - 0.16j)$ respectively, at frequency $F = 8.5$ GHz. Once again, the uncertainties on the complex permittivity appear larger in the ellipsometry method than in the Fresnel method.

D. Complex Permittivity Estimations Using Reflection Ellipsometry

The estimations of the complex permittivity of the different materials M2 to M6 lead to mean values of complex permittivities, as collected in Table I, as a function of frequency. The uncertainties associated to the real and the imaginary parts of $\tilde{\epsilon}_r$ are estimated to less than 15% and 30%, respectively; however, it is well known that the relative loss factor is quite difficult to estimate by free-space techniques, particularly when its value is lower than 0.5. Comparison of our measured values of relative complex permittivities with those reported in the literature in the case of similar materials characterized by other free-space techniques [3]–[9] confirms that the real parts of the relative permittivity belong to the ranges [2.1; 2.9] and [1.71; 2.5] for fiberboard and plasterboard, respectively, while relative loss factors belong to the ranges [0.04; 0.8] for fiberboard and [0.02; 0.1] for plasterboard; such results validate our estimations, but the relative loss factors appear higher. More generally, we observe that the real part of the permittivity has a higher value in the

case of thinner materials as reported in [8]. Moreover, samples of fiberboard ($e = 1.97$ mm) and PVC ($e = 2.15$ mm) have been characterized in a coaxial structure by P. Sabouroux at Université de Provence, France, leading to estimations of the complex permittivity versus frequency in the range [8 GHz; 18 GHz] [11]; the variations of the corresponding real parts are plotted in Fig. 12(a) and (b). We remark that these mean values agree with our estimations issued from reflection ellipsometry and that they fluctuate as a function of frequency. We do not provide the estimates of the loss factors ϵ_r'' issued from this method, because their uncertainties are not well characterized: they are mostly due to the manufacturing difficulty to produce a soft sample matching the guide without air-gap and to their low value (lower than 0.5 in the case of fiberboard and PVC samples).

Fig. 13 shows plots of the estimated real and imaginary parts of the complex permittivity averaged over several angles of incidence [35° , 40° , 45° , 50°], as a function of frequency, in the case of the thicker samples M3, M4, and M6. Fig. 14 reports the variations of the estimated complex permittivity in the case of the thinner samples M2 and M5 as a function of frequency. It appears that the complex permittivities of the different samples show fluctuations: considering the real part of the thicker fiberboard (M3) and plasterboard (M4) samples, they show in general an increase trend for the first case and a decrease trend

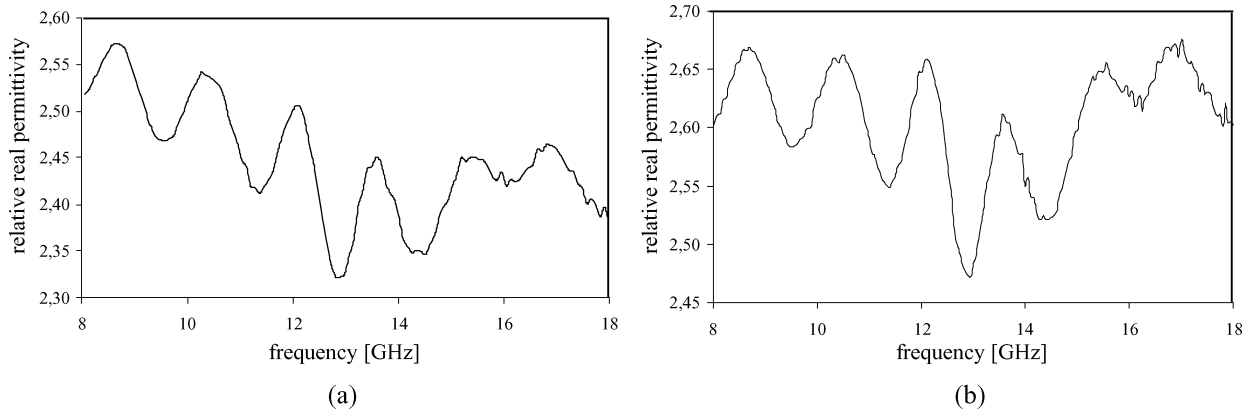


Fig. 12. Estimations of the real part of the complex permittivity of the (a) fiberboard and (b) PVC samples (thickness 1.97 and 2.15 mm, respectively) versus frequency in the range [8 GHz; 18 GHz] and issued from measurements made in a coaxial structure with a vector network analyzer (VNA).

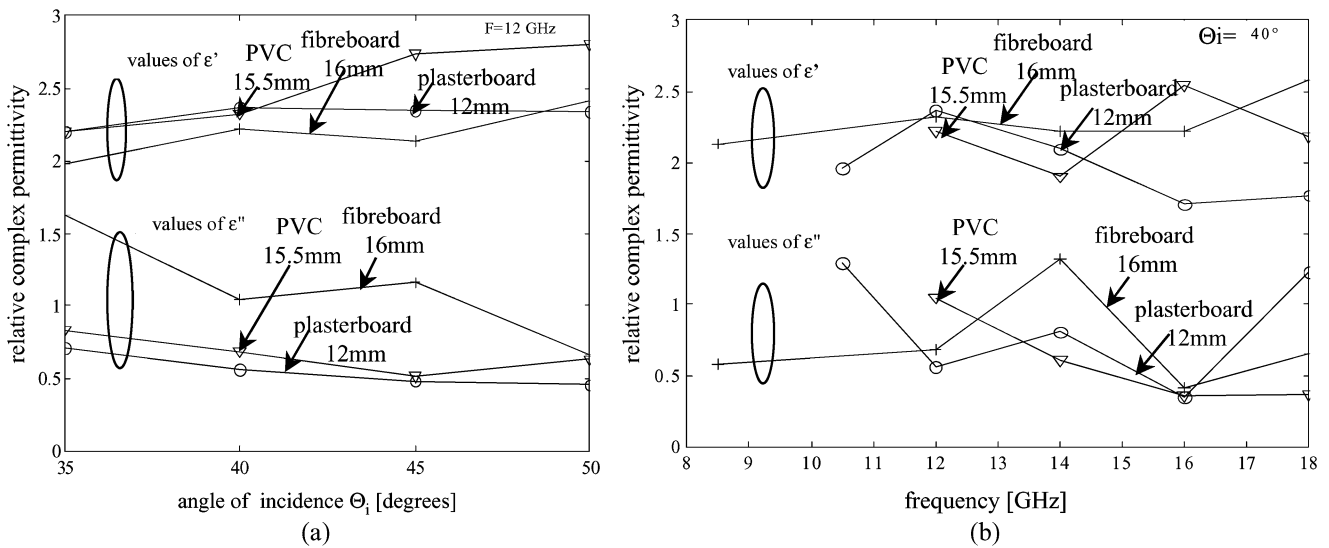


Fig. 13. Complex permittivity estimations for the thicker materials (PVC 15.5 mm, fibreboard 16 mm, and plasterboard 12 mm) (a) versus the angle of incidence in the range [35°; 50°] ($F = 12$ GHz) and (b) versus frequency in the range [8.5 GHz; 18 GHz] ($\Theta_i = 40^\circ$).

for the second one; such variations have already been observed by several authors [5], [6].

As a function of the angle of incidence, considering the three thicker samples at frequency 12 GHz. We observe in Fig. 13(a) that the variations of the complex permittivity of the 16-mm-thick fiberboard sample are smoother than for the 15.5-mm PVC and 12-mm plasterboard samples. However, the values remain close to the mean values collected in Table I.

IV. CONCLUSION AND PERSPECTIVES

We have designed a new *in situ* measurement setup that allows measuring, by reflection, the complex permittivity of common samples of arbitrary thicknesses, using two different methods and based on scalar only measurements. The influence of the relevant parameters, such as the angle of incidence and the frequency, on the shape of ellipsometric curves and on the estimation of the complex permittivity for the different samples has been studied, helping to understand thoroughly the experimental phenomena involved in reflection ellipsometry.

The conclusions of our approach are the following.

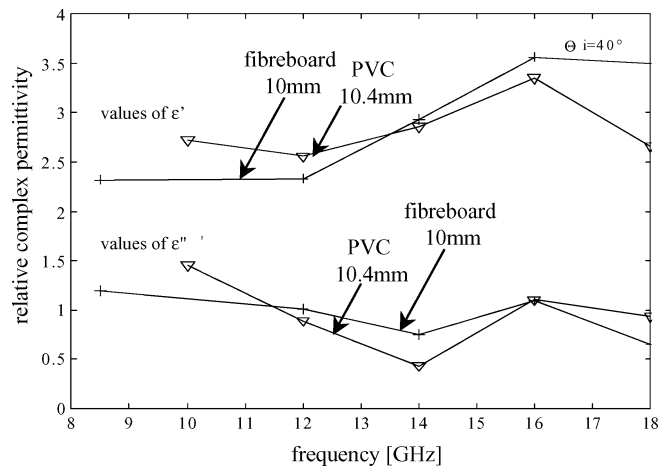


Fig. 14. Complex permittivity estimations for the thinner materials (PVC 10.4 mm, fibreboard 10 mm, and plasterboard 12 mm) versus frequency in the range [8.5 GHz; 18 GHz] ($\Theta_i = 40^\circ$).

- 1) From the experimental point of view, the Fresnel approach cannot be exploited on the whole range of angles of incidence, because of the Fresnel zone whose dimensions

vary with θ_i . On the contrary, in the case of ellipsometry, the angle of incidence can be judiciously chosen so as to optimize the measurement conditions. However, ellipsometry appears to be more sensitive to the adequacy between the geometrical parameters of the setup and the physical properties of the sample.

- 2) From the numerical point of view, the choice of the optimization method that determines the best fitting theoretical curve to the data is much more critical with the Fresnel approach. To our opinion, this results from the noisy characteristic of the measurement data generated by this method.
- 3) Concerning the results, the estimated complex permittivities, obtained from three different methods (ellipsometry, the Fresnel approach, and a guided structure) have been compared. They give real permittivity values which agree satisfactorily for the samples considered. The deviation between estimates of the loss factors is inherent to the free-space feature of the first two methods and to the manufacturing difficulty of the sample in the case of the last method. The estimated uncertainties associated with ellipsometry appear slightly greater than the Fresnel ones; we underline the fact that the uncertainty estimations are not evaluated using the same approach. Moreover, because of the nonconstant power of the direct path in the Fresnel method, it appears more difficult to fit the measurement curves in this approach.

As a conclusion, ellipsometry appears as a promising method that competes favorably with the Fresnel approach. Future developments include the extension of ellipsometry to broadband measurements, the study of the transmission configuration, of double-layer homogeneous samples, as well as of more realistic construction materials.

ACKNOWLEDGMENT

The authors would like to thank E. Rolland, M. Marques, and A. Akakpo for designing the experimental setup and conducting the measurements. The authors thank the reviewers for their valuable remarks about the manuscript.

REFERENCES

- [1] F. Sagnard, F. Bentabet, and C. Vignat, "In situ measurements of the complex permittivity of materials using reflection ellipsometry in the microwave band: theory (Part I)," *IEEE Trans. Instrum. Meas.*, vol. 54, no. 3, pp. 1266–1273, 2005.
- [2] F. Sagnard, D. Seetharamdoo, and V. Le Glaunec, "Reflection and transmission ellipsometry data analysis for measuring the complex permittivity of a single-layer material at microwave frequencies," *Microwave Opt. Technol. Lett.*, vol. 20, pp. 443–448, Jun. 2002.
- [3] J. P. Pugliese, A. Hammoudeh, and M. O. Al-Nuaimi, "Reflection and transmission characteristics of building materials at 62 GHz," in *Inst. Elect. Eng. Colloq. Radio Communications Microwave Millimeter Wave Frequencies*, 1996, pp. 6/1–6/6.
- [4] J. Lahteenmaki and T. Karttaavi, "Measurement of dielectric parameters of wall materials at 60 GHz," *Electron. Lett.*, vol. 32, no. 16, pp. 1442–1444, 1996.
- [5] L. Li, Y. Wang, and K. Gong, "Measurements of building construction materials at Ka-band," *Int. J. Infra. Millimeter Waves*, vol. 19, no. 9, pp. 1293–1298, 1998.
- [6] A. H. Muqabel. (2003, Mar.) Characterization of ultra wideband communication channels. [Online] <http://scholar.lib.vt.edu/theses/available/etd-03092003-095217/>
- [7] I. Cuinas and M. G. Sanchez, "Building characterization from complex transmittivity measurements at 5.8 GHz," *IEEE Trans. Antennas Propag.*, vol. 48, no. 8, pp. 1269–1271, 2000.
- [8] I. Cuinas, M. S. Varela, and M. G. Sanchez, "Wide band indoor radio channel measurements at 5.8 GHz," in *52nd IEEE Vehicular Technology Conf.*, vol. 2, 2000, pp. 695–702.
- [9] I. Cuinas and M. G. Sanchez, "Electromagnetic characterization of building materials at 5.8 GHz using transmission and reflection measurements," in *IEEE Antennas Propag. Soc. Int. Symp. Transmitting Waves Progress Next Millennium*, vol. 1, 2000, pp. 368–371.
- [10] C. A. Balanis, *Antenna Theory*, 2nd ed. New York: Wiley, 1997.
- [11] P. Sabouroux and J. P. Parneix, "A large bandwidth measurement system for the microwave characterization of absorbing materials," *J. Wave-Material Interact.*, vol. 7, no. 1, pp. 57–70, Jan. 1992.



Florence Sagnard was born in Paris, France, in 1965. She received the engineer diploma and the D.E.A. degree in electronics from Université Pierre et Marie Curie, France, in 1990 and the Ph.D. degree from Université d'Orsay, France, in 1996.

From 1990 to 1993, she was an Engineer on military electronic systems. From 1993 to 1996, she was with CEA and ONERA. Since 1997, she has been an Assistant Professor at Université de Marne-La-Vallée, France. Her research interests include microwave characterization of materials. In

September 2002, she joined IETR laboratory of INSA Rennes to devote her work to research on microwave and millimeter propagation inside buildings.

Faroudja Bentabet was born in France in 1978. She received the B.S.C. degree from Université de Marne-la-Vallée, France, in 2000 and the Ph.D. degree in mobile communications from Université de Versailles-Saint-Quentin, France, in 2001.

She is currently working in the telecommunication industry.



Christophe Vignat was born in France in 1965. He received the B.E.E. degree from Ecole Supérieure d'Electricité, Paris, France, and the Ph.D. degree in physics from Laboratoire des Signaux et Systèmes, Université de Paris-Sud, Orsay, France, in 1993.

Since 1995, he has been an Associate Professor at Université de Marne-La-Vallée, France. After working on adaptive systems, his interests shifted toward information theory and numerical methods applied to physics.